CONF-901105--28

SAND--90-1698C

DE91 004727

DEVELOPMENT OF INFRARED DETECTORS BASED ON TYPE II, InAsSb STRAINED-LAYER SUPERLATTICES

STEVEN R. KURTZ
Sandia National Laboratories, Albuquerque, New Mexico, 87185

Abstract

An overview is provided of long wavelength, photovoltaic detectors constructed with type II (also known as "staggered"), III-V superlattices. Specifically, the electronic properties of InAsSb strained-layer superlattices and prototype detectors utilizing these structures are described.

I. Introduction

Optical absorption in III-V semiconductors can be effectively extended to long wavelength ($\geq 10\ \mu m$) for infrared detector applications by utilizing low energy, intersubband transitions [1] or by reducing the superlattice valence-conduction bandgap with a type II band offset.[2] (We define a type II superlattice as a structure having the electron and hole potentials wells located in different layers of the superlattice.) The type II superlattice detectors potentially could fill a useful niche in long wavelength detector technologies. Type II detectors offer advantages for focal-plane-array construction because unlike intersubband detectors [3], type II detectors can operate as photodiodes, responsive to normal incidence light. Furthermore, the detectivity of type II detectors may soon rival that of HgCdTe while offering advantages to HgCdTe in manufacturability, durability, and radiation hardness.[4,5]

In this overview, the electronic and optical properties of type II, InAsSb/InSb strained-layer superlattices (SLS) are briefly summarized and compared with alternative, InAs/GaInSb type II SLSs. A high detectivity InAsSb SLS photodiode is described which illustrates both the potential of type II photodiode technologies and device design considerations for SLS detectors. Lastly, we speculate on the future directions of InAsSb detector development .

II. Electronic Properties of InAsSb SLSs and Other Type II Infrared Structures

In the mid-1970's, the InAs/GaSb superlattice was investigated as a near-lattice-matched alternative to GaAs/AlAs type structures. Immediately, the type II band offset in InAs/GaSb was identified [6], and the potential of type II superlattices for long wavelength infrared detectors was recognized. However, long wavelength optical absorption in InAs/GaSb superlattices was considered to be too weak for use as an infrared detector. With the development of lattice mismatched SLSs, Osbourn examined InAsSb SLSs as potential III-V structures having significant optical absorption at long wavelength.[7] Subsequently, a type II offset was discovered in these structures.[8,9]

A comparison of optical absorption in InAsSb SLSs and InAs/GaSb superlattices is shown in Figure 1. Both structures exhibit photoresponses extending to approximately 9 μm. Improved long wavelength absorption in InAsSb SLSs is clearly demonstrated in Fig. 1 although the SLS layers are roughly twice as thick as those of the InAs/GaSb superlattice. Because of the spatial separation of electrons and holes, absorption coefficients of type II superlattices at energies near the bandgap are sensitive functions of the superlattice layer thickness. The wavefunction overlaps which determine the strength of the band edge transitions depend on the exponentially decaying (evanescent) tails of the wavefunctions in the barrier layers. The decay lengths of these tails increase with decreasing barrier heights and decreasing effective masses. Useful absorption coefficients occur for decay lengths on the order of the barrier thickness, and band edge absorption in type II superlattices is increased by reducing layer thickness.

The relative bandgaps and barrier heights for InAs/GaSb and InAsSb SLSs are shown in Figure 2. The bandgaps of InAs and GaSb are much larger than that of InSb (See Fig. 2a), and the large barriers in InAs/GaSb superlattices result in the weak absorption seen in Fig. 1. Mailhoit and Smith proposed the use of InAs/GaInSb SLSs to increase the absorption coefficient from that of InAs/GaSb superlattices.[11] The bandgaps and barriers of a proposed InAs/GaInSb SLS are compared with that of an InSb/InAsSb SLS in Fig. 2b and 2c. The barriers in the InSb/InAsSb SLS remain significantly smaller than those of the InAs/GaAsSb SLS. This disadvantage is overcome by using very thin layers (< 40 Å) to increase absorption in InAs/GaAsSb SLSs. To obtain equal absorption coefficients and equal "cutoff" wavelengths in these two SLSs, the layers in the InAs/GaInSb SLS are thinner than those in the corresponding InSb/InAsSb SLS.

The energy levels of a typical InSb/InAsSb SLS are shown in Figure 3. (New magneto-optical and transport studies confirm this basic picture.[12]) Quantum size states have not been included in the figure. Characteristic of the type II, long wavelength SLSs, significant band edge absorption can result from electron minibands in the conduction band, and useful electron diffusion lengths, perpendicular to the SLS growth planes are easily obtained. Hole diffusion perpendicular to the growth planes is limited due to localization in the InSb layer of the lowest energy, out-of-plane heavy-hole (hh) state. Spatial separation of electrons and holes reduces band edge absorption in type II superlattices, but spatial separation also decreases electron-hole recombination rates. Long photocarrier lifetime increases the minority carrier diffusion length in photodiodes and can produce high gain in photoconductive detectors.

III. A High Detectivity, InAsSb SLS Photodiode

A high detectivity, SLS photodiode (Figure 4) was fabricated from a p-p$^-$-n junction embedded in an InSb/$InAs_{0.17}Sb_{0.83}$ SLS with equal, 150 Å thick layers. The p-n junction was formed during MBE growth; the p$^-$ doping resulted from background doping in the growth chamber. The photodiode was mesa-isolated, with an area of 1.2×10^{-3} cm ^{2}. Operation of the diode as a photodetector requires diffusion of minority carriers perpendicular to the SLS layers. Other details about the device have been described previously.[4]

The SLS material in the detector was very high quality, essentially dislocation free. This was confirmed by TEM and x-ray diffraction analysis. Consistent with high sample quality, an infrared photoluminescence line was observed at 9.7 µm (15 K sample temperature), with a 12 meV linewidth. The zero-bias resistance of the device was very sensitive to surface treatment, thus demonstrating that the detector noise was limited by surface leakage, not SLS material quality. After passivating the surface of the mesa with a native oxide, the resistance-area product (R_0A) increased from 0.6 to 9 $\Omega \cdot cm^2$ (77 K).

The zero-bias, external current responsivity (77 K) is shown in Figure 5. The detector was illuminated at normal incidence. Both the weak increase in responsivity observed in reverse bias and the magnitudes of the responsivity and absorption indicate that the minority carrier diffusion length, perpendicular to the SLS layers, is 1-2 µm. The detectivity values shown in Fig. 5 are based on a measured noise current of 1.6×10^{-12} $A/Hz^{1/2}$ at 100 kHz. These detectivity values surpass the 300 K BLIP limit, and the noise measurements were made with the detector covered by a 77 K cold-shroud. It is noteworthy that detectivities > 1 x 10^{10} cm $Hz^{1/2}$/W at wavelengths ≤ 10 μm were achieved with this passivated, photovoltaic InAsSb SLS detector.

IV. Future Directions of InAsSb Detector Development

The long wavelength, high detectivity photodiode in the previous section demonstrates the feasibility of an infrared detector technology based on InAsSb SLSs. Building on these results, it is conceptually straight-forward to improve the performance of these detectors. Detectivity can be increased by developing improved surface passivation techniques and by increasing the optically active volume while decreasing p-n junction area. A variety of novel device designs incorporating heterojunctions, lattice matched to the infrared active SLS, and lateral photodiode geometries may be used to increase detectivity. Many InSb microelectronic processing techniques can be transferred to InAsSb SLSs, and the spectral response of type II SLS detectors can be modified by changing SLS compositions and layer thicknesses.

The major obstacles to type II, SLS infrared detector development are associated with the immaturity of these III-V materials. We must demonstrate growth of high quality, infrared SLS wafers with excellent areal uniformity for focal-plane-arrays,and radiation-hard surface passivations must be developed. Like HgCdTe technology, the utilization of type II SLS detectors will be limited by material growth and microelectronic processing procedures and the manufacturability of these new technologies.

V. Acknowledgements

A large group has contributed to the infrared detector program at Sandia National Laboratories, and particularly, we thank R. M. Biefeld, L. R. Dawson, G. C. Osbourn, and R. E. Hibray for their enthusiasm and long-term collaboration on this project. This work was supported by DOE under contract No. DE-AC04-76P00789.

VI. References

1. L. C. West and S. J. Eglash, Appl. Phys. Lett. 46, 1156 (1985).
2. See for example, L. L. Chang and E. E. Mendez, in Synthetic Modulated Structures, edited by L. L. Chang and B. C. Giessen (Academic Press, New York, 1985) pp. 113-161.
3. B. F. Levine, C. G. Bethea, G. Hasnain V. O. Shen, E. Pelve, R. R. Abbott, and S. J. Hsieh, Appl. Phys. Lett. 56, 851 (1990).
4. S. R. Kurtz, L. R. Dawson, T. E. Zipperian, and R. D. Whaley, Jr., Elect. Dev. Lett. 11, 54 (1990).
5. S. R. Kurtz, J. G. Snyder, and L. R. Dawson, Proc. of the IRIS Specialty Group on Infrared Detectors, (in press) 1990.
6. G. A. Sai-Halasz, L. L. Chang, J. M. Wetter, C. A. Chang, and L. Esaki, Solid State Commun. 27, 935 (1978).
7. G. C. Osbourn, J. Vac. Sci. Technol. B2,176 (1984).
8. S. R. Kurtz, G. C. Osbourn, R. M. Biefeld, L. R. Dawson, and H. J. Stein, Appl. Phys. Lett. 52, 831 (1988).
9. S. R. Kurtz, G. C. Osbourn, R. M. Biefeld, and S. R. Lee, Appl. Phys. Lett. 53, 216 (1988).
10. D. K. Arch, G. Wicks, T. Tonaue, and J. Staudenmann, J. Appl. Phys. 58, 3933 (1985).

11. C. Mailhiot and D. L. Smith, J. Vac. Sci. Technol. A7, 445 (1989).
12. S. R. Kurtz and R. M. Biefeld, unpublished.

Figure Captions:

Figure 1 - Low temperature, optical absorption spectra for an $InAs_{0.13}Sb_{0.87}/InSb$ SLS (solid line, data from Ref. 8) with equal, 106 Å thick layers and an InAs/GaSb superlattice (dotted line, data from Ref. 10) with equal, 56 Å thick layers.

Figure 2 - (a) Relative energy levels of the conduction bands (C) and unstrained valence bands (L,H) of InSb, InAs, and GaSb. (b) Strained conduction band energies (C) and out--of-plane light-hole (L) and heavy-hole (H) energies for an $InAs/Ga_{0.6}In_{0.4}Sb$ SLS. (c) Strained conduction band (C) and valence band (L,H) energies for an $InAs_{0.2}Sb_{0.8}/InSb$ SLS. (Fig. 2a and 2b were obtained from Ref. 11.)

Figure 3 - Quantum well energies of an $InAs_{0.13}Sb_{0.87}/InSb$ SLS.

Figure 4 - Structure and composition of the InAsSb SLS photodiode.

Figure 5 - External current responsivity of the photodiode at zero-bias, 77 K. Detectivity was determined from noise measurements made at 100 kHz, cold-shielded at 77 K.

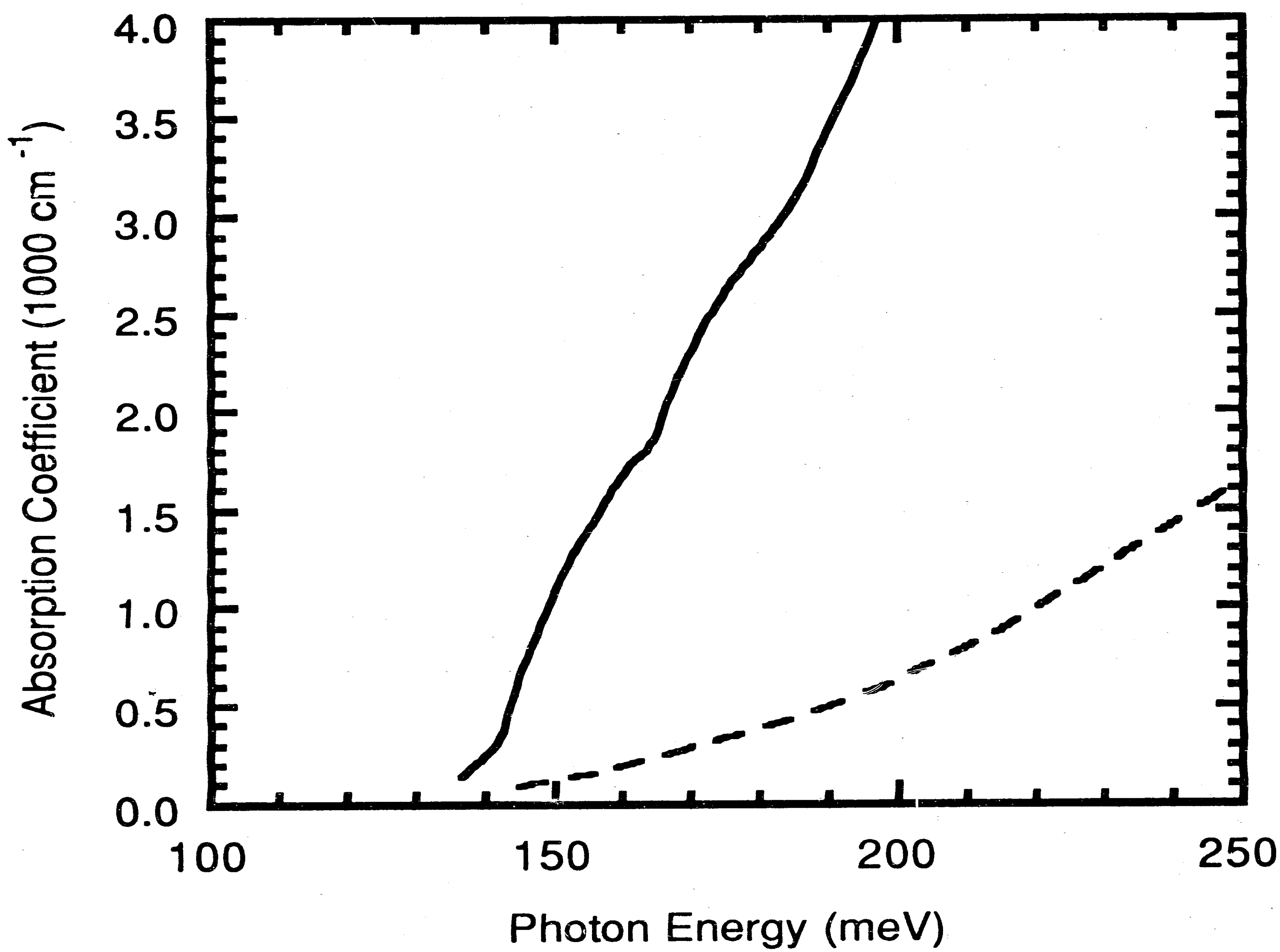

4.0
3.5
3.0
2.5
2.0
1.5
1.0
0.5
0.0
Absorption Coefficient (1000 cm -1)
100
150
200
250
Photon Energy (meV)

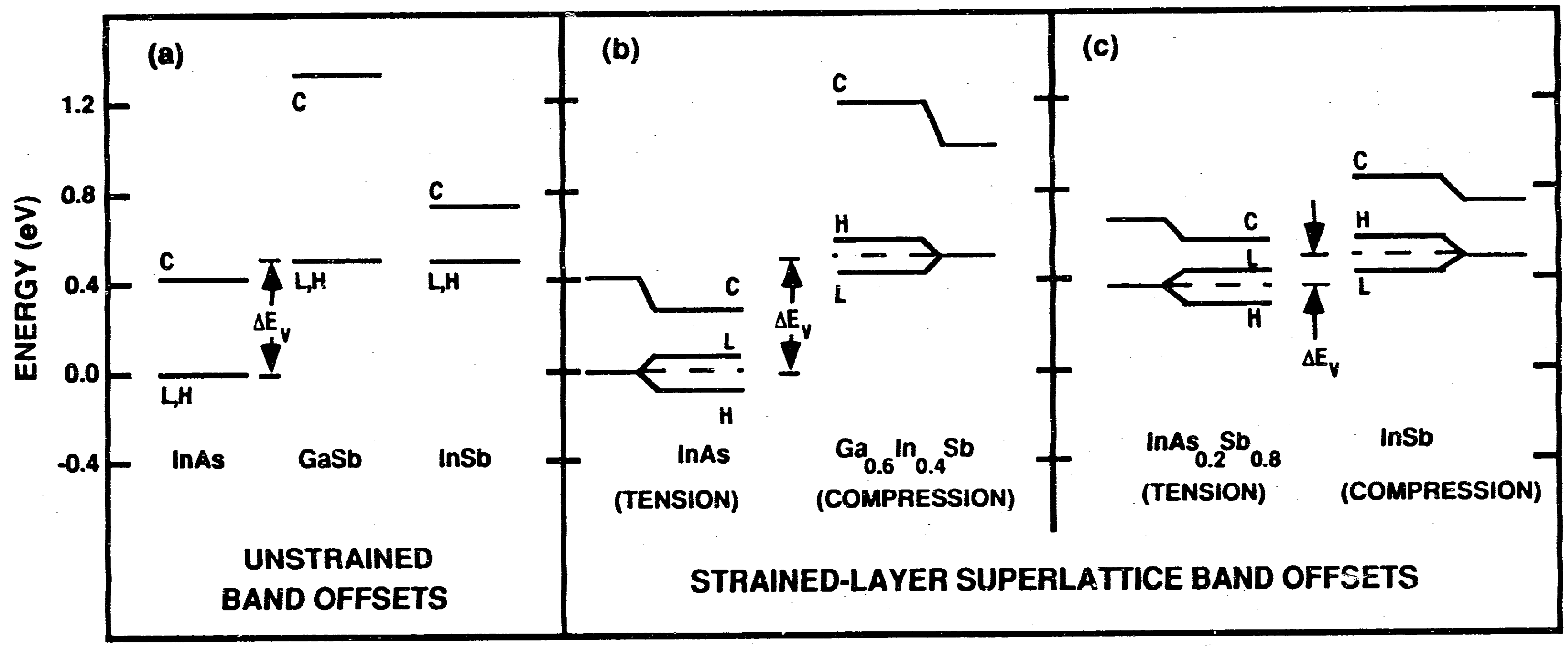
ENERGY (eV)
1.2
0.8
0.4
0.0
-0.4
(a)
C
L,H
ΔE_V
InAs
GaSb
InSb
UNSTRAINED
BAND OFFSETS
(b)
InAs
(TENSION)
Ga0.6In0.4Sb
(COMPRESSION)
(c)
InAs0.2Sb0.8
(TENSION)
InSb
(COMPRESSION)
H
L
STRAINED-LAYER SUPERLATTICE BAND OFFSETS

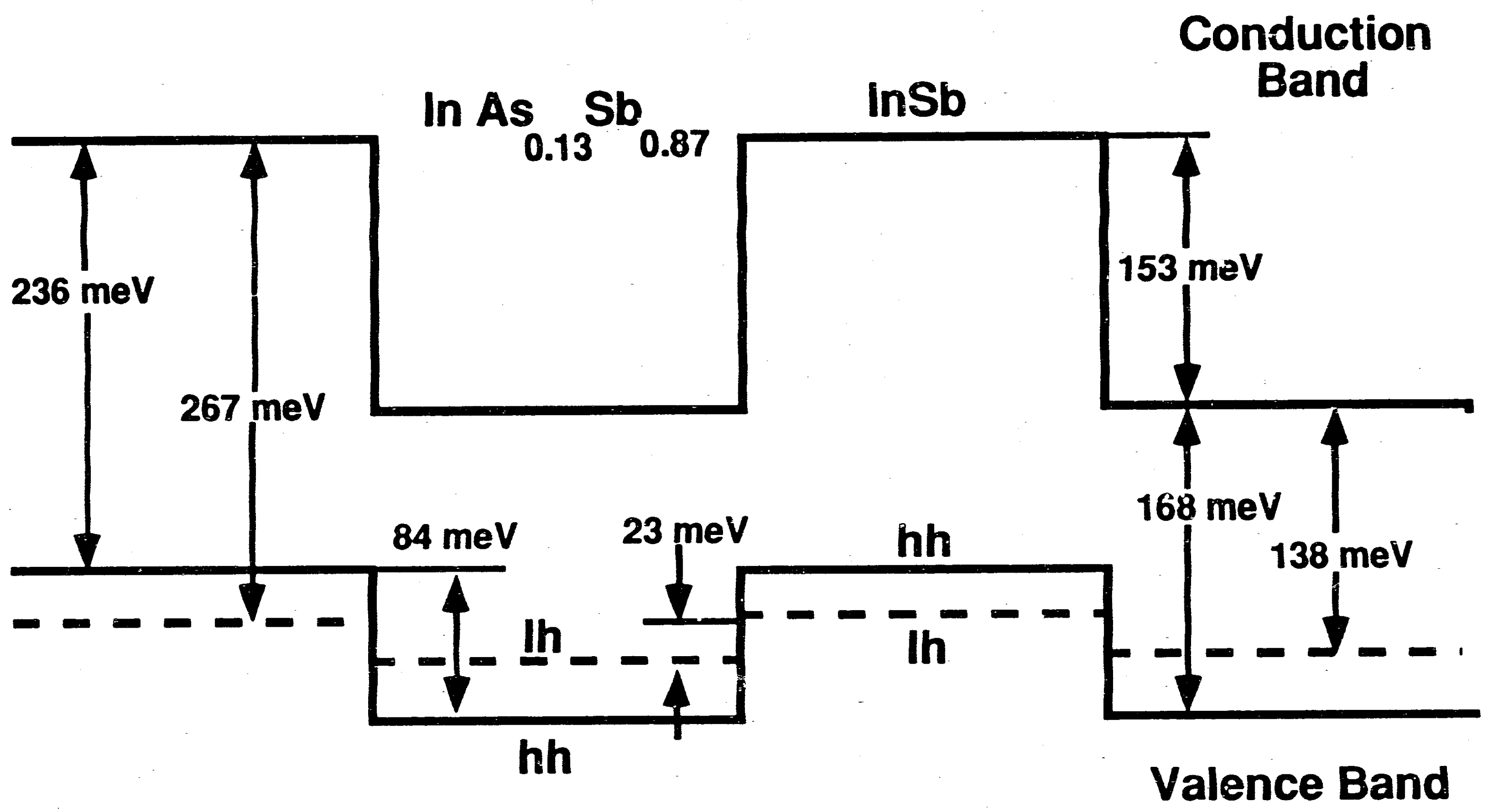

Conduction Band
In As 0.13 Sb 0.87
InSb
236 meV
267 meV
153 meV
168 meV
138 meV
84 meV
23 meV
hh
lh
lh
hh
Valence Band

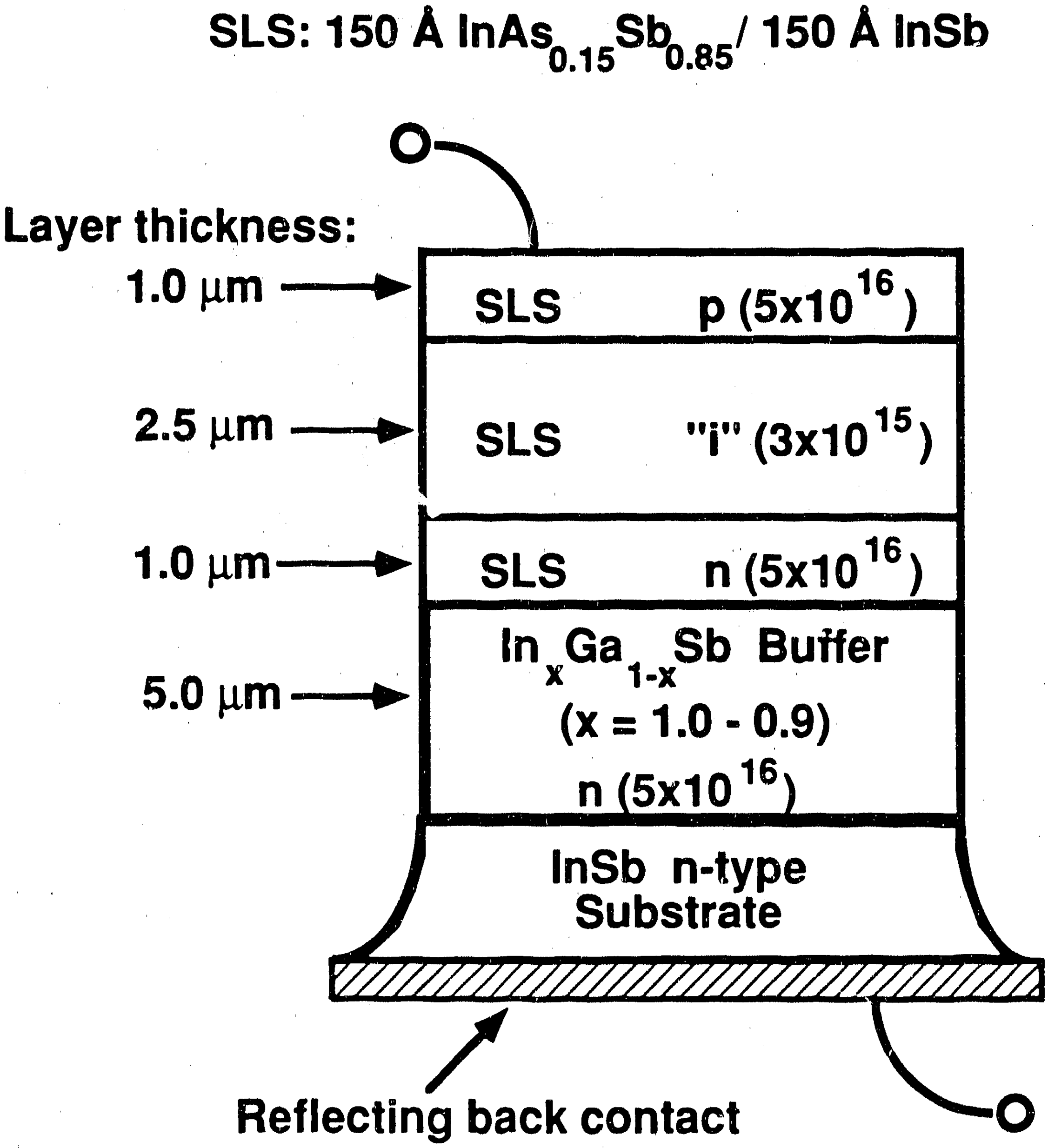
SLS: 150 Å $InAs_{0.15}Sb_{0.85}$/ 150 Å InSb
Layer thickness:
1.0 µm
2.5 µm
1.0 µm
5.0 µm
SLS p ($5x10^{16}$)
SLS "i" ($3x10^{15}$)
SLS n ($5x10^{16}$)
$In_xGa_{1-x}Sb$ Buffer
(x = 1.0 - 0.9)
n ($5x10^{16}$)
InSb n-type
Substrate
Reflecting back contact

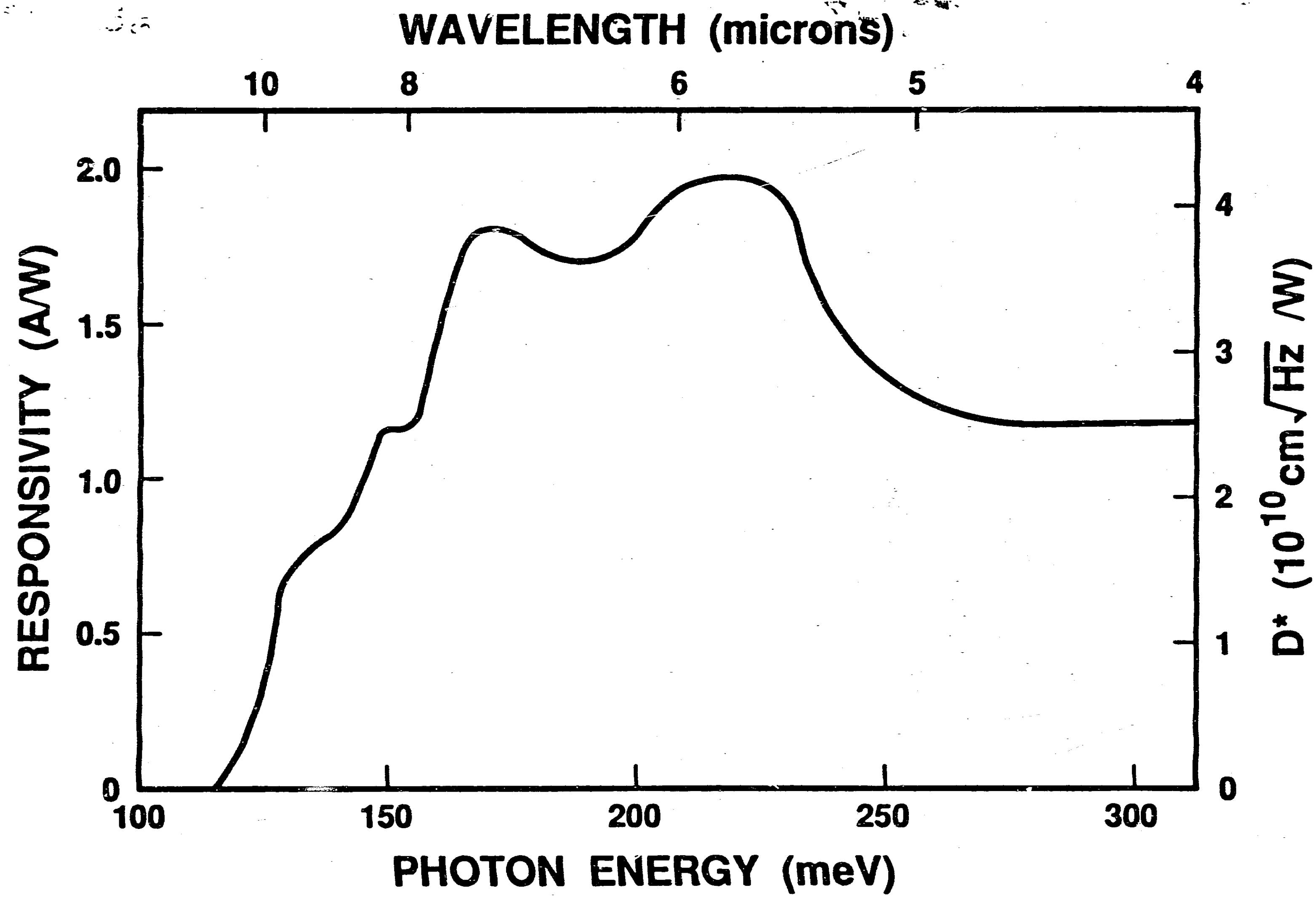
WAVELENGTH (microns)
10
8
6
5
4
RESPONSIVITY (A/W)
2.0
1.5
1.0
0.5
0
D* (10^{10}cm$\sqrt{Hz}$ /W)
4
3
2
1
0
100
150
200
250
300
PHOTON ENERGY (meV)

TA0042.02.01

END

DATE FILMED

01 / 23 / 91